Thermochimica Acta, 96 (1985) 239–258
Elsevier Science Publishers B.V., Amsterdam – Printed in The Netherlands

APPLICATION OF CALORIMETRY AND DTA TO METAL SYSTEMS *

GIACOMO BRUZZONE

Institute of Physical Chemistry, University of Genoa, Corso Europa, 30 Palazzo delle Scienze, 16132 Genova (Italy)

ABSTRACT

The calorimetric methods employed for the study of metal systems (solution, combustion, direct reaction calorimetry) are considered and briefly discussed with respect to each other.

The development of apparatus for the calorimetry of metals and alloys is examined as a whole, with particular reference to the progressive increase of the maximum limit of the working temperature.

The employment of calorimetric methods for the determination of equilibrium phase diagrams is described according to two different approaches:

(1) corresponding to classical DTA, based on the identification of phase boundaries by the exploration of the system as a function of temperature, at constant composition;

(2) corresponding to the measurement of partial and integral enthalpies of alloy formation as a function of the composition, at constant temperature.

A brief report is given of the utilization of calorimetric data for the computation of equilibrium phase diagrams and equations are also given that allow the equilibrium temperature to be calculated between a liquid solution (binary or multicomponent) and a pure component (or an intermetallic compound) as a function of the thermodynamic parameters obtained by calorimetric methods.

INTRODUCTION

Calorimetric methods enable different goals to be attained in the study of metallic systems:

(1) experimental determination of equilibrium phase diagrams;

(2) direct measurement of thermodynamic quantities, such as enthalpy of formation, mixing and phase change of alloys;

(3) direct measurement of heat content as a function of temperature and determination of heat capacity by derivation with respect to temperature.

They also contribute to:

(1) the predictive computation of equilibrium phase diagrams;

* Presented at the International Summer School of Calorimetry and Thermal Analysis, 1–5 October 1984, Belgirate, Italy.

0040-6031/85/$03.30

(2) the calculation of thermodynamic quantities, such as, free mixing and free formation enthalpies.

The foundations of alloy calorimetry are described in several books [1–3]. Surveys of the development of experimental alloy thermochemistry have been presented by Komarek in 1973 and 1977 [4,5], Kubaschewski in 1981 [6], and Predel in 1982 [7]. In these papers, various methods of calorimetry and second-law methods (i.e., measurement of electromotive forces or dissociation pressures) have been reviewed and compared.

With regard to calorimetry, three methods can be listed: solution, combustion, and direct reaction.

Solution calorimetry

Initially, solution calorimetry measurements were attempted at or near room temperature, employing aqueous inorganic solvents, such as, hydrochloric acid, for intermetallic compounds in fairly simple calorimeters, e.g., Bunsen-type ice calorimeter. The results obtained, however, are open to excessively large errors, because, when working with alloys, the heats of formation are measured as relatively small differences of large heats of solution and great precision is required. Thus, aqueous solution calorimetry was quickly found to be an unsatisfactory approach to the study of alloys, and metallic solvents have subsequently been used with fairly good results at high temperatures:

(1) liquid tin, employed in different versions of a suitable calorimeter described by Ticknor and Bever [8];

(2) liquid aluminium, as designed by Mathieu et al. [9];

(3) liquid copper and liquid copper alloys [10,11];

(4) liquid nickel and iron [12] for even higher temperatures;

(5) liquid manganese–nickel alloy (40% Ni), used by Kleppa and Hong [13] for determination of the formation enthalpy of metallic carbides.

Generally speaking, the working temperature for such calorimeters must be well above the melting point of the solvent metal to ensure the abundant solubility of the solute. However, the number of thermodynamic data obtained in these ways is still small. As Kleppa [14] observed, it is very regrettable that this approach has not been pursued more actively in recent years.

Combustion calorimetry

In combustion calorimetry, too, the results are made up of small differences of large quantities and the same objections apply. Only in the case of strongly exothermic compounds, such as those formed by metals with semimetal elements, can this method be employed, but especially using fluorine [15,16] rather than oxygen, because metal fluorides generally deviate less from the stoichiometry than oxides.

This gives better results, because measurement of the change in temperature on mixing liquid metals, for example, in more or less sophisticated calorimeters, involves an error which is much smaller than that in computing the heats of formation from solution or combustion heats using Hess's law. The great advantage of this method, especially when the water equivalent is large, was recognized at an early stage. Direct reaction calorimetry is generally applied to liquid–solid and liquid–liquid reactions. However, other cases can also be investigated: Gerdanian, for example [17], measured, with a high-temperature version of the Tian–Calvet calorimeter, the partial enthalpy of oxygen in non-stoichiometric metal oxides.

With regard to their operating temperature range, calorimeters are of two ideal types: isothermal and adiabatic. However, another type of calorimeter has been designed for high-temperature operations. This is the heat flux calorimeter, in which the total integral heat flux can be conveniently and reproducibly measured. Application of the isothermal method to temperatures higher than 100°C is generally not to be recommended, owing to the rapid loss of heat by radiation. The adiabatic method should be used, since there is no heat interchange between the calorimeter and its surroundings, and so there is no correction to apply to the observed temperature difference.

CALORIMETERS

Some basic apparatus can be mentioned.

(1) The calorimeter made by Kawakami [18] for determination of the heat of mixing of liquid metals was employed for low-melting point alloys. The water equivalent of this apparatus was rather low.

(2) The isothermal calorimeter of Oelsen and Middel [19] was employed for determination of the heat of formation of silicides and aluminides of transition metals (iron group). The experiment required two or three operators! The error, in the model of Oelsen and Kubaschewski, was about 6%. The rise of temperature in the cell had to be offset by heating with an electric circuit, so that a zero electromotive force occurred in a series of thermocouples connected differentially to a galvanometer.

(3) The Ticknor–Bever [8] tin–liquid apparatus for measurements of heat of solution for low-melting point metals up to 320°C. The error was 5%, especially due to the slight formation of tin oxide (having a high heat of formation) which could not be prevented.

(4) The adiabatic calorimeter designed by Kubaschewski and Evans [1] for metallurgical reactions, which could operate up to 700°C with an error of 2.5%.

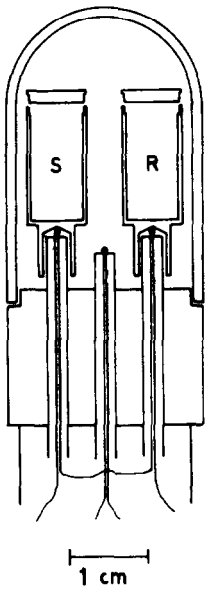

Fig. 1. Crucible assembly for dynamic differential calorimetry (S = sample; R = reference) [24].

(5) The heat flux calorimeter designed by Kleppa [20] for temperatures below 500°C. It was based on the same principle as Calvet and Prat's microcalorimeter [21], which, like the Tian–Calvet [22] apparatus, was employed for extensive work on the heats of formation of alloys up to 1200°C.

(6) The Tian–Calvet calorimeter [22], in which more than a hundred thermocouples in series are used to achieve maximum sensitivity. Among the models derived from this apparatus, a commercial version has been prepared by Setaram Co. (Lyon, France), which works up to 1700 K [23].

In the last ten years, several high-temperature differential scanning calorimeters (DSC) have been used and made available commercially, like the Tian–Calvet apparatus. The DSC [3] derives from the DTA and an integrated heat flux device is also employed. However, in this case heat flux integration is carried out over a range of temperature. Owing to the high sensitivity of the method, only small quantities of sample are required. The error may be around 1%, as for the Tian–Calvet calorimeter.

Dynamic differential calorimetry (DDC) has also been employed in the past and is still used. With this method, measurements of heats of formation of a series of rare earth intermetallic compounds were carried out at the Institute of Physical Chemistry, University of Genoa [24]. Figures 1 and 2 show, respectively, the crucible assembly and the reciprocal sensitivity of the apparatus, based on the formula suggested by Facktor and Hanks [25].

The heat of formation of a compound can be measured during the direct reaction. Working with an apparatus with good sensitivity, the result is likely

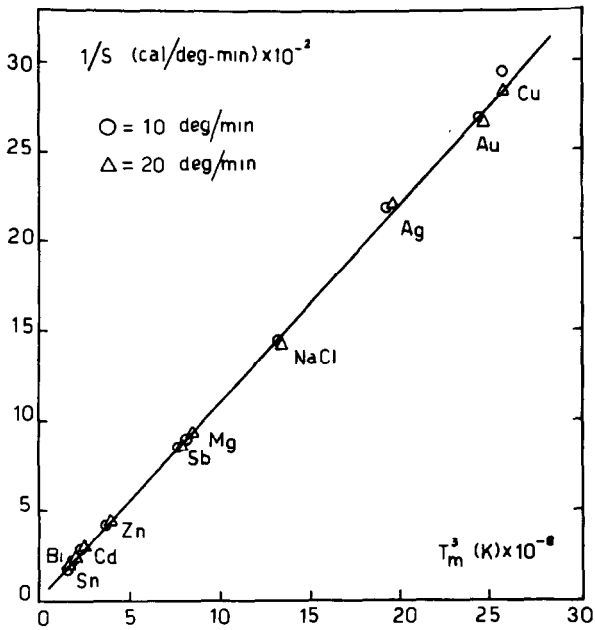

Fig. 2. Reciprocal sensitivity against the cube of absolute temperature: $1/S = H/(\int_0^t \Delta T \mathrm{d}t) = A + BT_m^3$, where $\int_0^t \Delta T \mathrm{d}t$ = peak area; A, B = constants containing the transmission coefficients for conduction and radiation; T_m = temperature of the central thermocouple for the peak area divided into equal parts [25].

to be more accurate than when employing solution calorimetry or other methods. The validity of the results is obviously limited to the case of complete reaction between the powders of the two metal components.

Another calorimeter, based on the same condition, has been recently designed by Hertz and Gachon [26]. It can work between 1000 and 1800 K.

With the more resistant materials now available, the operational temperature of direct reaction calorimeters has been raised to 1900–2000 K, and in some cases to even higher values. However, for alloys of the refractory metals with other metal partners, a strongly exothermal reaction can also occur, so that very high operational temperatures are not always reached.

An adiabatic calorimeter which works at 1900 K was designed by Kubaschewski and Dench [27,28] and afterwards improved by several workers [29,30]. Its essential parts are made of alumina. Compacts of metal powder mixtures are heated adiabatically from a certain temperature, called the "safe temperature", to the reaction temperature and the heat effect is recorded. The experiment is repeated with the reacted alloy. The difference in the heat contents gives the heat of formation at the "safe temperature". Working with the same metal A/metal B ratio in unalloyed specimens, the difference gives the heat of formation at the reaction temperature. The

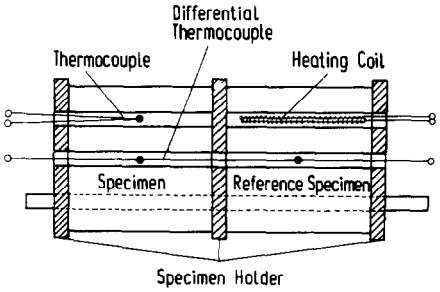

Fig. 3. Experimental arrangement for the Hoster and Kubaschewski calorimeter [30].

equations corresponding to this procedure are the following

$$A(T_0) + B(T_0) \rightarrow AB(T); \qquad h_R \tag{1}$$

$$AB(T_0) \rightarrow AB(T); \qquad \Delta^T_{T_0} h(AB) \tag{2}$$

$$A(T_0) + B(T_0) \rightarrow A(T) + B(T); \qquad \Delta^T_{T_0} h(A + B) \tag{3}$$

where T_0 = safe temperature and T = reaction temperature. So, one can obtain, from eqns. (1) and (2), and (1) and (3), respectively

$$h^f(T_0) = h_R - \Delta^T_{T_0} h(AB)$$

$$h^f(T) = h_R - \Delta^T_{T_0} h(A + B)$$

A calorimeter derived from the model of Kubaschewski and Dench is that of Hoster and Kutase [31]. Figure 3 shows two cylindrical specimens of similar heat capacity (test and reference) in the tube resistance furnace, with a differential thermocouple with its junctions in the middle of each specimen and a thermocouple for the measure of the absolute temperature. The calibration is made with a Pt coil, which can be placed in a bore in the test

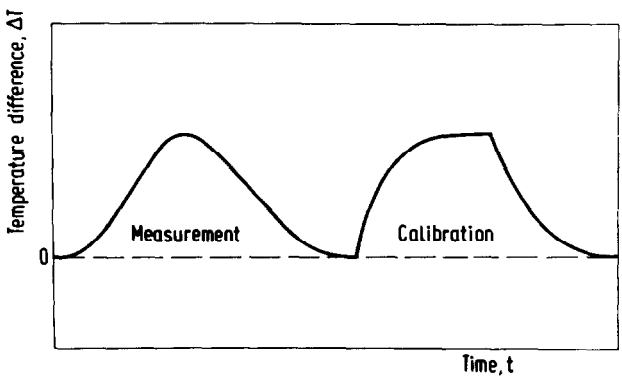

Fig. 4. Measurement and calibration curves of the calorimeter reported in Fig. 3.

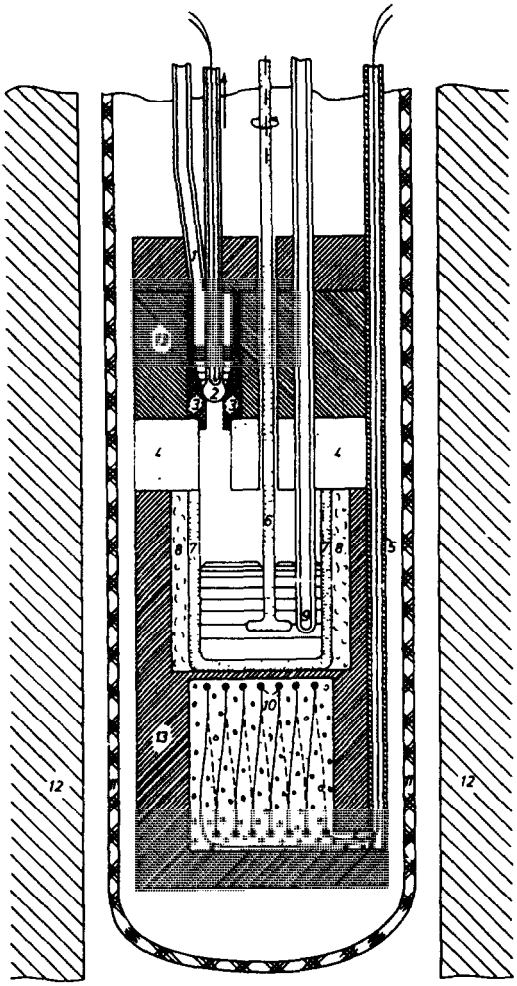

Fig. 5. High-temperature calorimeter for determination of mixing and solution enthalpies according to Oehme and Predel [32]: (1) charging tube; (2) plug; (3) melting crucible; (4) refractory material ring; (5) protective tube for the thermopile conducting leads; (6) stirrer; (7) reaction tube; (8) thermal insulation; (9) calibration tube; (10) thermopile; (11) outer tube; (12) furnace; (13) thermal blocks.

specimen and produces an accurate, known quantity of heat, choosing the heating current and the time so that the areas under the measurement and calibration curves are about equal, as shown in Fig. 4.

Another example of a simple high-temperature calorimeter, derived from the Ticknor–Bever type, is shown in Fig. 5. It has been made by Oehme and Predel [32]. In addition to determining the integral mixing enthalpy of liquid alloys (Fig. 6), it allows good determination of the derivative of Δh_{mix} as a function of the concentration. The values of mixing enthalpy thus obtained can be accurate to 1%. If, in the place of the liquid component, the solid

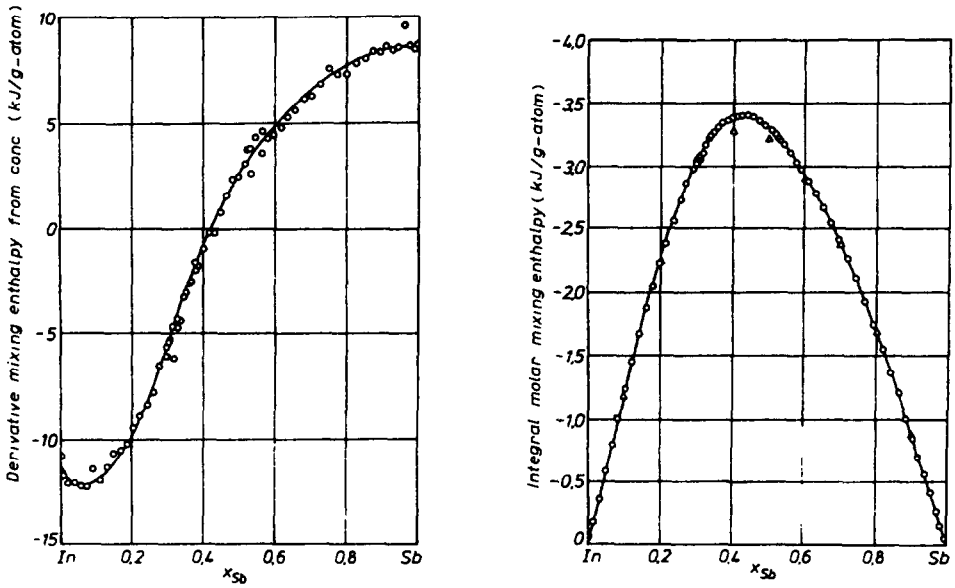

Fig. 6. (A) $d\Delta H/dx - x$ curve for liquid In–Sb alloys at 953 K. (B) $\Delta H - x$ curve for liquid In–Sb alloys [32].

substance to be investigated is dropped into a metallic solvent present in the crucible, the solution enthalpy of solid alloys can be determined as well as the formation enthalpy.

A calorimeter applied to mixing enthalpy measurements of liquid alloys, operating up to 2000 K, has recently been made by Lück and Predel [33] (Fig. 7).

Above 2000 K, since for heat content determinations it is now possible to employ drop calorimetry involving levitation of the melting sample, an apparatus for mixing enthalpy measurements has been designed by Frohberg and Betz [34]. The central part of this calorimeter is shown in Fig. 8. The two metals are melted separately in two levitating fields. The mixing of the two components is obtained by short-circuiting some windings of the coil and the ΔT value of the alloy is measured pyrometrically. This value of ΔT gives the mixing enthalpy. Figure 9 shows the mixing enthalpy of Nb–Si alloys obtained at 3000 K. The errors are around 10%.

The upper limit of about 3000 K for the levitation technique is due to the loss for thermal radiation, which becomes too high above this temperature.

At higher temperatures up to 8000 K, as Gathers et al. [35] report for tantalum, a method has been proposed which again allows the melting enthalpy of solids to be obtained. The experiment is very short, to eliminate the losses cited. The solid to be investigated, in the form of a wire, is supported within a cell filled with He or Ar to a pressure of 0.4 GPa to increase the boiling point by high pressure. During the experiment

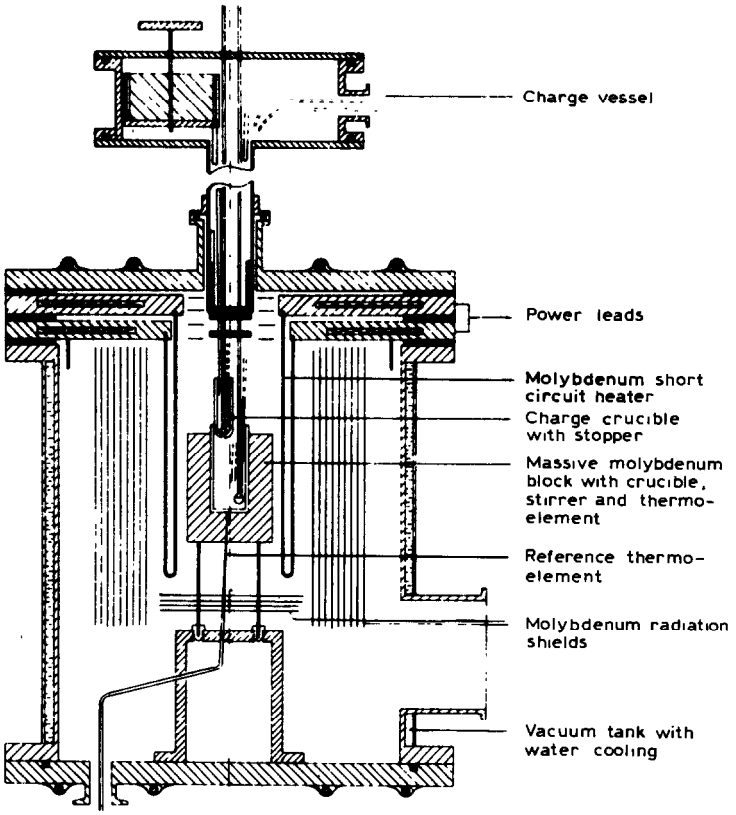

Fig. 7. High-temperature calorimeter according to Lück and Predel [7,33].

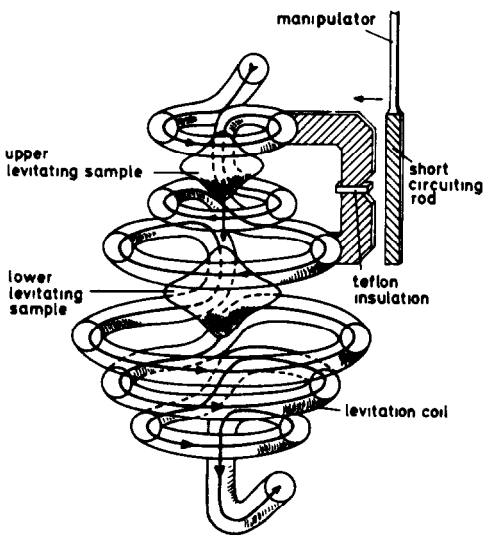

Fig. 8. Central part of the calorimeter of Frohberg and Betz: levitation coil with two levitating samples before mixing [34].

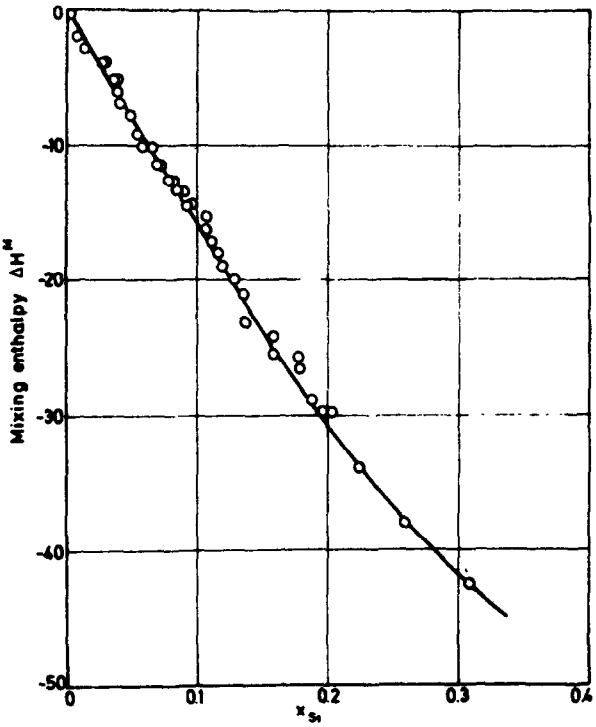

Fig. 9. Integral mixing enthalpy of liquid Nb–Si alloys [34].

($\leqslant 100$ μs), the wire maintains its cylindrical shape and is heated to about 8000 K with a very high current pulse (30 kA). A series of 20 kV condensors is used to give a total energy of 60 kJ. The dilatation of the wire is measured with a laser beam, the shadow of the wire being recorded photographically. The change in temperature is measured pyrometrically. The experimental values are made up of the changes of volume and of temperature of the wire. The error reported for tantalum measurements up to 4250 K is 3%.

EQUILIBRIUM PHASE DIAGRAMS BY DTA

Determination of equilibrium phase diagrams through differential thermal analysis is so simple in concept that time, on the foundations of this method, may be saved.

If one is lucky, the results are unambiguous. For the hypothetical binary system represented in Fig. 10, for example, DTA would give the signals shown and a check of the thermal data by metallographic and X-ray analysis enables the diagram to be drawn correctly [36]. Yet even in DTA misleading results can occur. The main reason is generally a condition of non-equilibrium for the particular composition. A classic example is shown in Fig. 11,

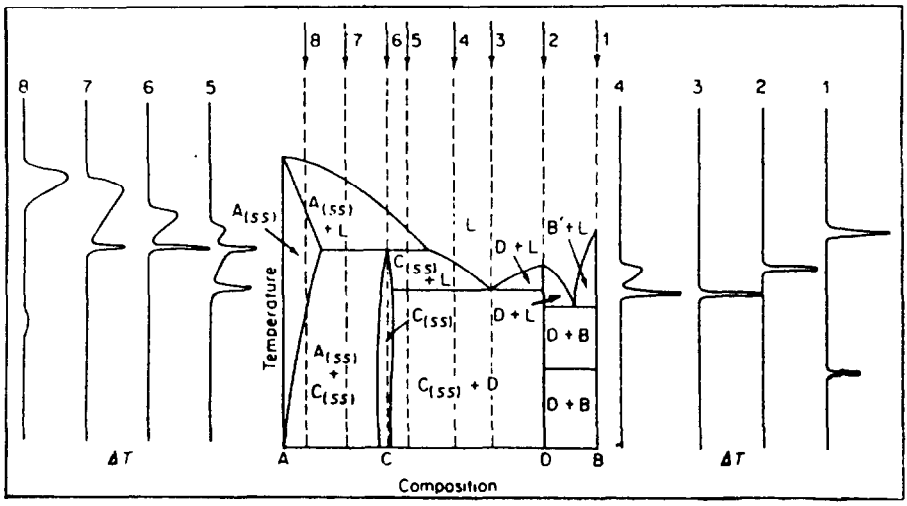

Fig. 10. Representation of DTA curves likely to be obtained at various compositions in the hypothetical system A–B (ss = solid solution) [36].

corresponding to a part of the Sn–Cd system [37]. The β-phase is formed on heating by a peritectic at approximately 130°C. The first set of data presented spurious thermal effects at 158–167 and 176°C, persistent in the regions of the single β-phase and the β- + α-Sn phases, due to inhomogene-

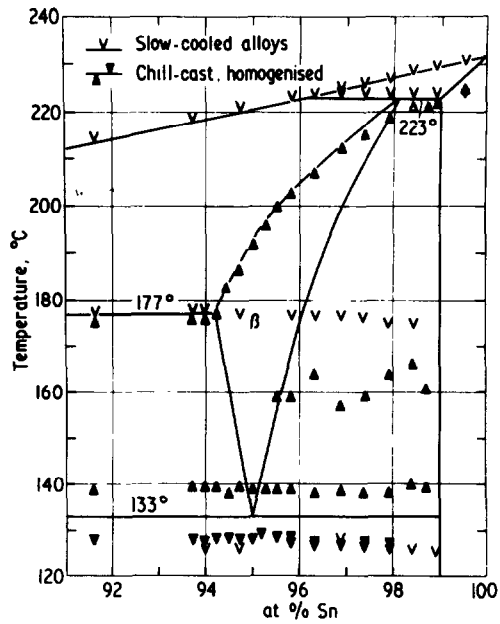

Fig. 11. Part of the Cd–Sn system with spurious thermal effects [37].

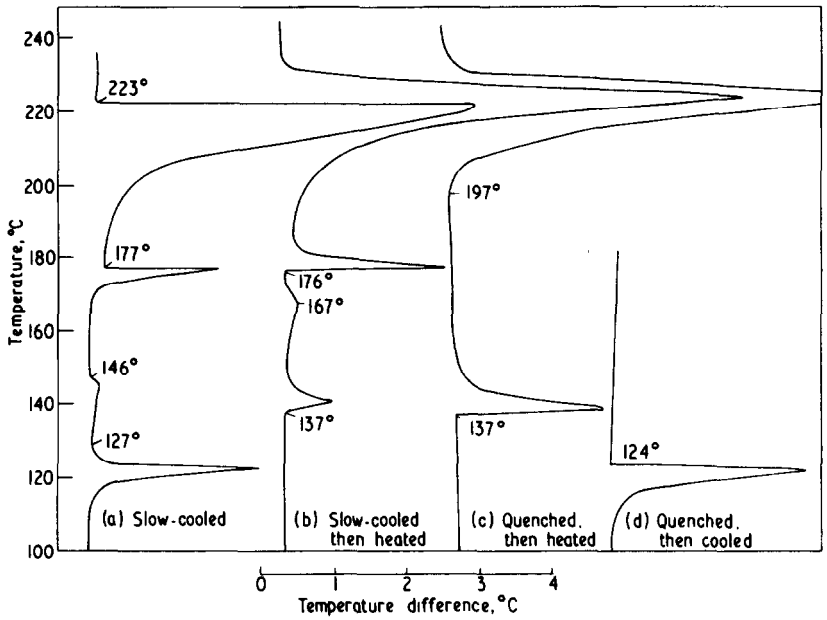

Fig. 12. DTA curves for the Cd–95.5 at% Sn alloy in the slow-cooled and quenched conditions [37].

ity that also occurs when the alloys are slowly cooled. Consequently, the other thermal effects registered in DTA must also be regarded with suspicion, because in this case the alloy sample may be split into portions of different composition. For ternary alloys, the work may become even more difficult. The best precaution is to prepare samples of homogeneous composition.

Figure 12a and b shows that DTA curve of the composition 95.5 at% of Sn, for which the signals at 177 and 146°C should not be present, since the alloy was cooled at 1°C min^{-1}. Other experiments show that neither cycling the slow-cooled alloy through the spurious arrest nor prolonged heat-treatments eliminate the trouble. The explanation consists of a coring reaction (structures of non-equilibrium) associated with precipitation of the β-phase: the β-phase is unable to change in composition at a good rate within the time scale of the DTA.

The results are better if the samples are quenched from above the liquidus, as shown in Fig. 12 c and d, because the rapidly cooled alloys are free from lag-scale segregation and are therefore more readily converted at equilibrium by some heat treatment. In this manner, the coring reaction and the associated spurious thermal effects can be eliminated or very considerably reduced (Fig. 13). In most cases, a cooling rate of a few hundred degrees per minute is adequate. Each of the solid-state reactions could be then defined in heating and cooling runs before the more complicated solid–solid reactions were investigated.

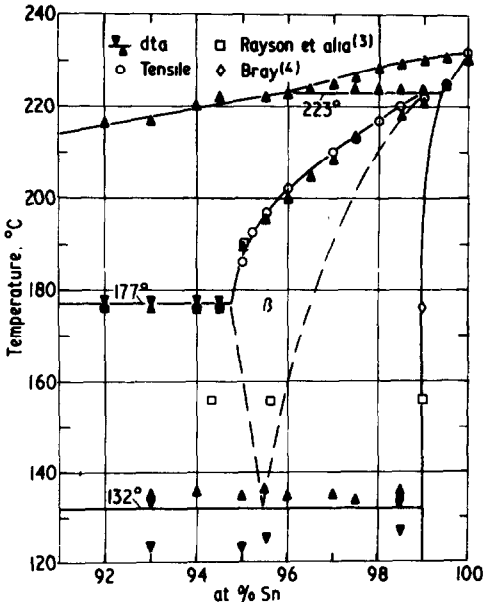

Fig. 13. As Fig. 11: results with quenched alloys.

This method is the classic approach generally employed by direct measurements made in the vertical crossing of phase boundaries (in parallel direction to the temperature, at constant pressure).

Yet another method in which both calorimetry and DTA play fundamental roles was introduced by Castanet et al. some years ago [38]. The partial and integral enthalpies of formation of alloys are measured versus mole fraction at a constant temperature, and the phase boundaries are then obtained horizontally in the phase diagram. Figure 14 shows a relatively simple case of an equilibrium phase diagram for a system in which only one intermediate phase, congruently melting, exists. Let us consider the equilibrium at the temperature T and examine the integral molar enthalpy of formation of the A-alloys based on both liquid components at this temperature versus the mole fraction, x_B. We will find a trend such as that reported in Fig. 14, where the integral enthalpy is linear with respect to the mole fraction x_B in the two-phase regions BC and DE. Moreover, if the partial molar enthalpy of formation of the component B is represented vs. the mole fraction x_B, also shown in Fig. 14, at the crossing of the phase boundary this quantity undergoes a discontinuity which will permit its localization.

The balance for every drop of component B in the solvent bath, the integral molar enthalpy of formation at the temperature T, and the partial enthalpy of mixing of B with respect to x_i are calculated as reported in the Appendix. When the experimental temperature is lower than the melting points of the two components, the integral enthalpy of formation of the

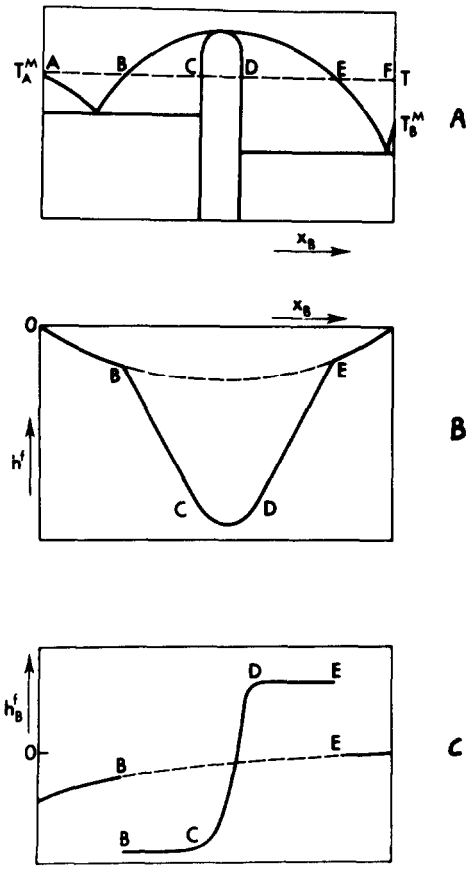

Fig. 14. (A) Phase diagram of the A–B binary system. (B) Integral molar enthalpy of formation of A–B alloys at temperature T vs. mole fraction of B. (C) Partial molar enthalpy of formation of component B at temperature T vs. mole fraction of B [38].

liquid phase is no longer obtained. However, it is possible to measure the partial enthalpies of the two components by dropping these in a liquid master alloy prepared outside. The integral enthalpy of formation is then calculated from the following relation

$$h^{f} = xh_{A}^{f} + (1-x)h_{B}^{f}$$

In the work of Castanet et al., determination of the boundaries and enthalpies of formation of the solid compound and intermediate phases is possible, as shown in Fig. 15, when the integral molar enthalpy of formation of the A–B alloys (with reference to both pure liquid components) is reported vs. x_A at a certain temperature. In the Pb–Te system, for example, $T = 737$ K and a strong minimum for $x_{Pb} = 0.5$ corresponds to a straight-line compound and not to the absolute phase diagram shown on the left of Fig. 15 and taken from Hansen and Anderko's compilation [39].

If the measurements for the enthalpy of formation of a solid phase are

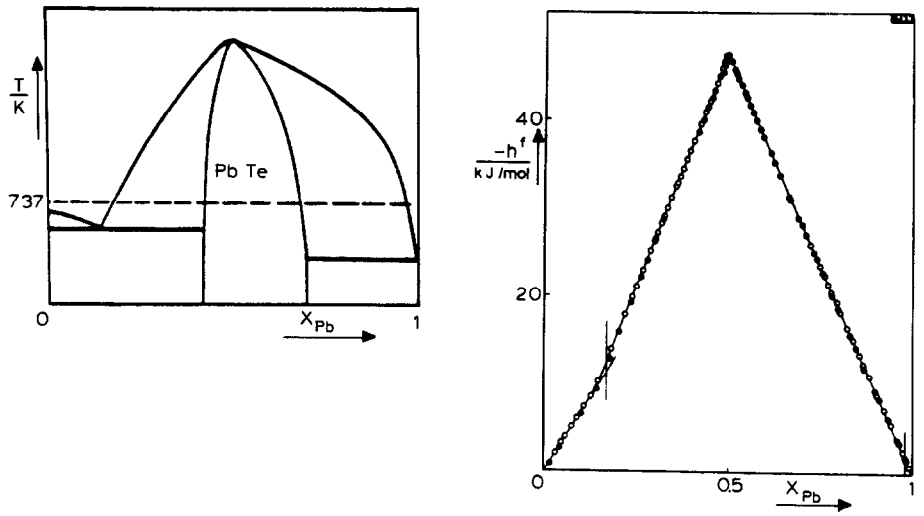

Fig. 15. Integral molar enthalpy of formation of the Pb–Te alloys at 737 K with reference to both pure liquid components [38].

carried out at different temperatures, the heat capacity of the compound itself can be obtained. Moreover, by measuring the enthalpy of formation immediately above the melting point, the melting enthalpy is also available. Finally, the results reported by Castanet et al. employing direct calorimetry

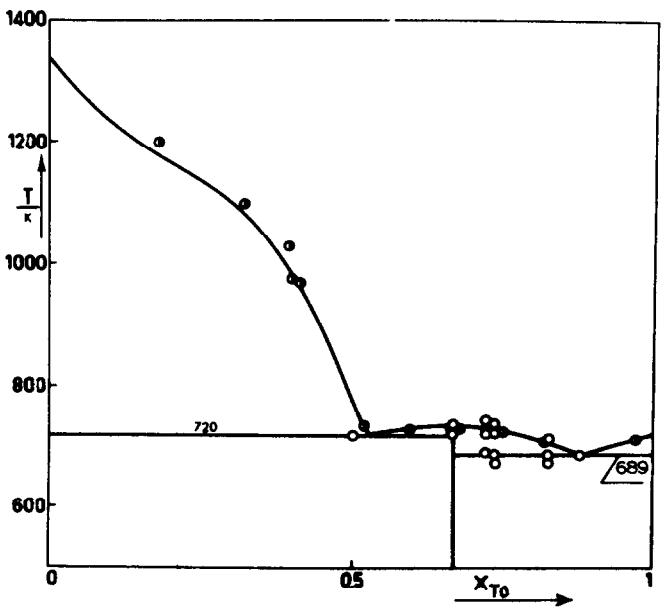

Fig. 16. Phase diagram of the Au–Te system: the lines represent the literature diagram; (◑) results by direct reaction calorimetry; (○) results by differential thermal analysis [38].

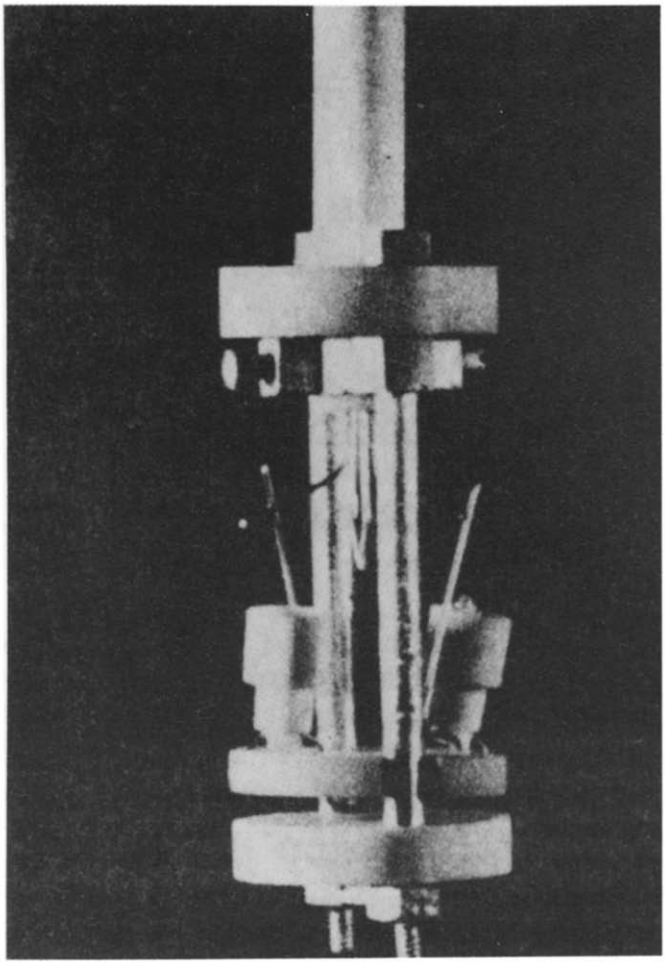

Fig. 17. DTA sample holder with two BeO crucibles (5 mm diameter) [40].

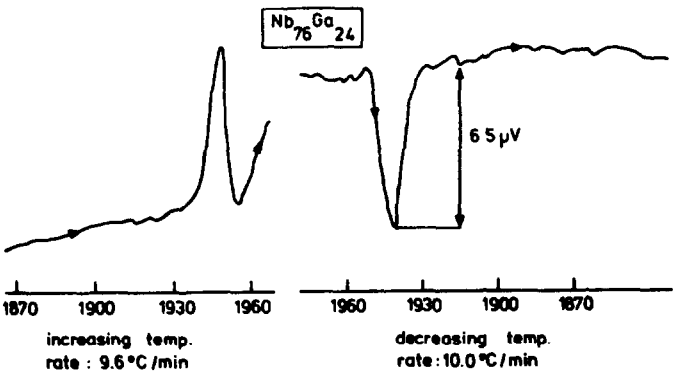

Fig. 18. DTA run of $Nb_{0.76}Ga_{0.24}$ at 4 atm [40].

and DTA for the Au–Te system are shown in Fig. 16 as examples of the agreement of all the available information, because the lines are those reported in the literature.

For the determination of partial and integral enthalpies, calorimeters able to measure small heat quantities must be employed, such as the micro-calorimeter of Tian–Calvet, following the drop method.

With regard to high temperatures, a DTA apparatus working up to 2200°C under an inert gas pressure of up to 10 atm, required for phase diagrams of superconducting materials with volatile components, was made by Flükiger [40], who studied Nb-alloys. The best material for the heating resistance is tungsten, but it becomes brittle by recrystallization and reacts with oxygen, so carbon was preferred. By giving the carbon resistance a particular complex shape, a homogeneous temperature of 2200°C was kept in a zone of about 40 mm length, with a gradient of 0.5°C cm^{-1}. The cells were made of BeO and molybdenum was used for the cylindrical box in which they were placed. Figure 17 shows the DTA sample holder. The weight of the crucibles was comparable to that of the samples (0.2–0.25 g). Figure 18 reports a DTA run of $Nb_{0.76}Ga_{0.24}$ at 4 atm with a strong curvature of the baseline due to initial evaporation on increasing temperature. At high temperature, the possibility of reaction of the alloy components with the crucible must always be checked. Levitation thermal analysis (LTA) completely eliminates this problem [41,42].

COMPUTATION OF BINARY PHASE DIAGRAMS BY CALORIMETRIC DATA

From a computing point of view two methods are known:

(1) calculating the limits of all the possible two-phase regions as a function of the temperature and then deriving the equilibrium phase diagram from stability considerations;

(2) calculating the Gibbs energy of all possible diphasic fields at a given temperature and over all compositions, retaining only the phase combination giving the lowest Gibbs energy.

Both approaches are open when thermodynamic data are available for all solution phases and intermetallic compounds in the system.

The following examples show the utilization of the calorimetric data [43].

(1) When one has to define the liquidus line representing the phase boundary between a liquid solution in equilibrium with a solid element, the following equation can be used

$$T = (\Delta\bar{H}_i + L_i)/(\Delta\bar{S}_i + L_i/T_i)$$

where $\Delta\bar{H}_i$ and $\Delta\bar{S}_i$ are the partial enthalpy and entropy of mixing for component i, and L_i and T_i are the enthalpy and temperature of melting of component i.

(2) When the liquid solution is in equilibrium with an intermetallic compound, the liquidus temperature is represented (from the fundamental equation based on the partial Gibbs energy of a component in each of the phases in equilibrium) as follows

$$T = \frac{x\left(\Delta\bar{H}^{l}_{A}\right)_{x} + (1-x)\left(\Delta\bar{H}^{l}_{B}\right)_{x} - \Delta H_{C} + xL_{A} + (1-x)L_{B}}{x\left(\Delta\bar{S}^{l}_{A}\right)_{x} + (1-x)\left(\Delta\bar{S}^{l}_{B}\right)_{x} - \Delta S_{C} + \dfrac{L_{A}}{T_{A}} + (1-x)\dfrac{L_{B}}{T_{B}}}$$

where x = molar fraction of A in the compound C; $\Delta\bar{H}^{l}_{A}$, $\Delta\bar{H}^{l}_{B}$ = partial enthalpies of mixing of A and B in the liquid solution, respectively; $\Delta\bar{S}^{l}_{A}$, $\Delta\bar{S}^{l}_{B}$ = partial entropies of mixing of A and B in the liquid solution, respectively; ΔH_{C}, ΔS_{C} = partial enthalpy and entropy of formation of the compound C, respectively; L_{A}, T_{A} = enthalpy and temperature of fusion of the component A, respectively; L_{B}, T_{B} = enthalpy and temperature of fusion of the component B, respectively.

This equation is also valid if a multicomponent liquid phase is in equilibrium with a pure metal or with a binary intermetallic compound, and can be used to calculate the liquid surface.

Moreover, it can be generalized to the equilibrium between a multicomponent system containing m components and an intermetallic compound, formed of k constituents ($k < m$), provided that the enthalpy and entropy of formation (or their enthalpy of fusion) are known.

APPENDIX

Balance for every drop of B in the solvent bath

$$n_{i}\mathrm{B}(s,T_{0}) + N_{i-1}\mathrm{All.}(T,x_{i-1}) - (N_{i-1}+n_{i})\mathrm{All.}(T,x_{i}) \qquad \text{(A1)}$$

where n_{i} = molar quantity of B added at the ith addition to the bath; $N_{i-1} = n_{A} + \sum_{1}^{i-1} n_{i}$ = molar quantity of the bath after the $(i-1)$th addition of B; x_{i} = molar fraction of the component B after the ith addition; x_{i-1} = molar fraction of the component B after the $(i-1)$th addition; n_{A} = molar quantity of A placed in the cell before any addition of the component B.

Integral molar enthalpy of formation at T

$$h^{f}_{i} = \left(\sum_{1}^{i} H_{i} - h^{*}_{B}\sum_{1}^{i} n_{i}\right) \Big/ \left(n_{A} + \sum_{1}^{i} n_{i}\right) \qquad \text{(A2)}$$

where H_{i} = enthalpy of the reaction (1); $h^{*}_{B} = h_{B}(T) - h_{B}(T_{0}) + \epsilon h_{\mathrm{fus\,B}}$; with $\epsilon = 1$ when $T < T_{\mathrm{fus}}$ and $\epsilon = 0$,when $T > T_{\mathrm{fus}}$.

Partial enthalpy of mixing of B with respect to x_i

$$h_B^f(x_i) = (H_i - h_B^* n_i)/n_i \tag{A3}$$

Note: $h_A(T)$ and $h_B(T)$ for calibration of the apparatus and for calculation of $h^f(x_i)$ referring to liquid components are taken from the available chemical data tables.

REFERENCES

1 O. Kubaschewski and E.L. Evans, Metallurgical Thermochemistry, Pergamon Press, London, 1958.
2 R.C. Mackenzie, Differential Thermal Analysis, Vols. I and II, Academic Press, London, 1970 and 1972.
3 W.W. Wendlandt, Thermal Methods of Analysis, 2nd edn., Wiley, New York, 1974.
4 K.L. Komarek, Z. Metallkd., 64 (1973) 325.
5 K.L. Komarek, Ber. Bunsenges. Phys. Chem., 81 (1977) 936.
6 O. Kubaschewski, Physica, 103B (1981) 101.
7 B. Predel, Calphad, 6 (1982) 199.
8 L.B. Ticknor and M.B. Bever, J. Met., 4 (1952) 941.
9 J.C. Mathieu, B. Journel, P. Desrè and E. Bonnier, in Proc. IAEA Symp. Thermodynamics of Nuclear Materials, Vienna, 1967, p. 767.
10 M.G. Benz and J.F. Elliott, Trans. Metall. Soc. AIME, 230 (1964) 706.
11 R.D. Dokken and J.F. Elliott, Trans. Metall. Soc. AIME, 233 (1965) 1351.
12 F. Woolley and J.F. Elliott, Trans. Metall. Soc. AIME, 239 (1967) 1872.
13 O.J. Kleppa and K.C. Hong, J. Chem. Thermodyn., 10 (1978) 243.
14 O.J. Kleppa, in Y.A. Chang and J.F. Smith (Eds.), Calculation of Phase Diagrams and Thermodynamics of Alloy Phases, AIME, Washington, DC, 1979, p. 213.
15 H. Feder et al., in Proc. IAEA Symp. Thermodynamics of Nuclear Materials, Vienna, 1967, p. 1872.
16 P. Gros, C. Hayman and J.T. Bingham, Trans. Faraday Soc., 62 (1966) 2388.
17 P. Gerdanian, in Coll. Int. CNRS No. 201, Thermochemie, Marseille, 1971.
18 M. Kawakami, Sci. Rep. Tohoku Imp. Univ., 16 (1927) 915; 19 (1930) 521.
19 W. Oelsen and W. Middel, Mitt. Kaiser-Wilhelm-Inst. Eisenforsch., Dusseldorf, 19 (1937) 1.
20 O.J. Kleppa, J. Phys. Chem., 59 (1955) 175.
21 E. Calvet and H. Prat, Microcalorimetrie, Masson, Paris, 1956.
22 R. Castanet and J.C. Mathieu, J. Therm. Anal., 28 (1983) 259.
23 R. Castanet, R. Chastel and C. Bergman, J. Chem. Thermodyn., 15 (1983) 773.
24 A. Palenzona and S. Cirafici, in R.S. Porter and J.F. Johnson (Eds.), Analytical Calorimetry, Vol. 3, Plenum Press, New York, 1975, p. 743.
25 M.M. Facktor and R. Hanks, Trans. Faraday Soc., 63 (1967) 1122.
26 J.C. Gachon and J. Hertz, Calphad, 7 (1983) 1.
27 O. Kubaschewski and W.A. Dench, Acta Metall., 3 (1955) 339.
28 W.A. Dench, Trans. Faraday Soc., 59 (1963) 1279.
29 R. Ferro and R. Capelli, Atti Accad. Naz. Lincei, 34 (1963) 659; R. Ferro, R. Capelli and A. Borsese, Thermochim. Acta, 10 (1974) 13.
30 K. Hack and H.D. Nüssler, Bedienung Sauleitung: Adiabatisches Hoch-temperaturekalorimeter, Lehrstuhl für theorische Huttenkunde, Techn. Hochschule, Aachen, 1979.

31 J. Hoster and O. Kutase, Thermochim. Acta, 40 (1980) 15.
32 G. Oehme and B. Predel, Thermochim. Acta, 22 (1978) 267.
33 R. Lück and B. Predel, Z. Metallkd., 73 (1982), cited in ref. 7.
34 M.G. Frohberg and G. Betz, Arch. Eisenhütten., 51 (1980) 235.
35 G.R. Gathers, J.W. Shammer and R.L. Brier, Rev. Sci. Instrum., 47 (1976) 471.
36 W. Gutt and A.J. Majumdar, in R.C. Mackenzie (Ed.), Differential Thermal Analysis, Vol. II, Academic Press, London, 1972, Chap. 29.
37 D.S. Evans and A. Prince, Thermochim. Acta, 58 (1982) 199.
38 R. Castanet, C. Bergman and J.C. Mathieu, Calphad, 8 (1979) 62.
39 M. Hansen and K. Anderko, Constitution of Binary Alloys, McGraw-Hill, New York, 1958.
40 R. Flükiger, in S. Forrer and B.B. Schwartz (Eds.), Superconducting Materials Science: Metallurgy, Fabrication and Applications, NATO Summer School, Sintra, 1980, Plenum Press, London, 1981.
41 R. Flükiger and J.L. Jorda, in M. Carter (Ed.), Application of Phase Diagrams in Metallurgy and Ceramics, National Bureau of Standards Spec. Publ. 196, Washington, DC, 1978, p. 375.
42 J.L. Jorda, R. Flükiger and J. Muller, J. Mater. Sci., 13 (1978) 2471.
43 I. Ansara, Comparison of Methods for Thermodynamic Calculation of Phase Diagrams, Lecture held at the workshop: Giornate Genovesi di Metallurgia, University of Genoa, Genoa, Italy, 1981.